A&A 375, 113–121 (2001)
DOI: 10.1051/0004-6361:20010809

Astronomy & Astrophysics

20 CVn: A monoperiodic radially pulsating δ Scuti star*

M. Chadid[1,2], J. De Ridder[3], C. Aerts[3], and P. Mathias[1]

[1] Observatoire de la Côte d'Azur, UMR 6528, BP 4229, 06304 Nice Cedex 04, France
[2] European Southern Observatory, Alonso de Cordova 3107-Vitacura, PO 19001 Santiago, Chile
[3] Katholieke Universiteit Leuven, Instituut voor Sterrenkunde, Celestijnenlaan 200 B, 3001 Leuven, Belgium

Received 19 March 2001 / Accepted 30 May 2001

Abstract. We present a new spectroscopic study of the δ Scuti star 20 CVn in order to solve the controversy on the type of pulsation mode of this object. The spectra were obtained at the Observatoire de Haute-Provence, with the Echelle spectrograph ELODIE. Using the correlation configuration of the instrument, sinusoidal moment variations are clearly detected, with a frequency in perfect agreement with the photometric one. Using the moment method, we conclude that only the radial mode is able to explain the observed moment variations and leads to a good fit to the observed line profiles. The new data thus allow us to confirm the photometric results, i.e. 20 CVn exhibits a monoperiodic radial pulsation.

Key words. stars: oscillations – stars: variables: δ Scuti – stars: individual: 20 CVn

1. Introduction

Delta Scuti stars are located in the classical instability strip and are characterized by small amplitude, short-period light and radial velocity variations. We refer to Breger (2000) for a review. Most of the low-amplitude δ Scuti stars have rather complicated variation curves, interpreted as the result of the simultaneous excitation of several pulsation modes, both radial and non-radial. Therefore, these stars are potential targets for asteroseismology (e.g. Templeton et al. 2000).

Quite a large number of stars in the δ Scuti instability strip turn out to be constant. It remains a question if this is physically real or merely a consequence of the detection treshold. Neither do we know if multiperiodicity – a prime condition for asteroseismology to work – is always present. There are some indications that the amplitudes of many modes are indeed below the current detection treshold (Breger 2000). Firstly, the number of δ Scuti stars strongly increases with decreasing amplitude. Secondly, theoretical models predict several hundreds of unstable modes, which is about a factor of ten higher than what is currently observed photometrically (e.g. Bradley & Guzik 2000). The amplitude-limiting mechanism acting in δ Scuti stars is presently unknown, but it is thought to be different from the one in large-amplitude pulsators like Cepheids and RR Lyrae variables (Gautschy & Saio 1996). In this context, seemingly monoperiodic δ Scuti stars are interesting since there the amplitude discrimination appears to be largest. A mode identification for these stars may be useful to constrain the theoretical models of the amplitude-limiting mechanism.

We have taken the initiative to gather spectra for the seemingly monoperiodic δ Scuti star 20 Canum Venaticorum (= HD 115604, hereafter 20 CVn) to find out in what kind of mode it pulsates. 20 CVn is a bright ($V = 4.73$) δ Scuti star of spectral type F3III. We refer to an earlier paper on 20 CVn by two of us (Mathias & Aerts 1996), for a list of references concerning 20 CVn. For our purposes it is sufficient to say that all authors find a clear first frequency and some suspect a second one. Up to now all mode identifications obtained via spectra point towards a non-radial mode for the main frequency. The most recent spectroscopic mode identification was done by Mathias & Aerts (1996) who obtained a non-radial primary mode with $\ell = 3$ or 2, and $|m| = 2$. The most recent photometric mode identification was done by Rodríguez et al. (1998) who obtained 831 Strömgren measurements during 8 nights. Fourier analysis led to a unique peak at $8.2168\,\mathrm{cd}^{-1}$, with no residual signal above 5 mmag. The mode identification based on phase shifts and amplitude ratios between the observed light and colour variations (Garrido et al. 1990) showed no good agreement between pulsation theory and observations, but the authors nevertheless gave solid arguments to derive a radial mode.

The aim of this paper is first of all to solve the controversy between the recent photometric and spectroscopic results for 20 CVn by analysing a large new dataset of

Send offprint requests to: M. Chadid,
e-mail: mchadid@eso.org

* Based on observations obtained at the Observatoire de Haute Provence.

high-quality spectroscopic data. Moreover, we seek an answer to the question whether or not 20 CVn has more than one low-amplitude mode. The new observations are described in Sect. 2. In Sect. 3 an analysis of the radial velocities is given, while Sect. 4 concerns the mode identification by means of both the moment method and line-profile fitting. Finally, some conclusions are given in Sect. 5.

2. Observations

The spectroscopic observations were made with the cross-dispersed spectrograph ELODIE (Baranne et al. 1996) of the 1.93 m telescope of the Observatoire de Haute-Provence. The detector was a 1024×1024 elements CCD.

Two series of spectra were obtained: on April 11, 12, 13 and 14 in 1998 and on April 24, 27, 28 and 29 in 1999. In total, 268 spectra ranging from 3900 Å to 6800 Å were measured with a resolution of $R = \lambda/\Delta\lambda = 37\,000$. The typical exposure time was around 6 min, resulting in an average signal-to-noise ratio of 150.

The spectra were reduced on-line, using the INTER-TACOS software (see Baranne et al. 1996) which takes care of the offset and flat-field pixel-to-pixel corrections, as well as the wavelength calibration in the heliocentric frame. This latter operation is done by means of a simultaneous exposure on both the star and a thorium lamp which is possible through the presence of two optic fibers. Such a procedure ensures an absolute precision for the velocity better than 100 m s^{-1}.

The spectrum can be normalized to the continuum, and individual (low S/N) lines can be considered, or directly correlated with a given mask, as in the case of CORAVEL (Baranne et al. 1979). The correlation was computed with one of the electronic spectra provided by INTER-TACOS, which corresponds to an F0V star, a spectral type slightly different from the one of 20 CVn, the latter being F3 III (Rodríguez et al. 1994). The noise level of the correlation profile is very low, since more than 2000 lines are involved for its computation. We will emphasize later on that the computation of the correlation profile with the purpose of mode identification is a delicate matter and should be done with much caution.

3. Frequency analysis on the radial velocity

The radial velocity curves related to the two seasons 1998 and 1999 are respectively represented in Figs. 1 and 2. Both series show a very nice sinusoidal shape, as is usually noted for this star whatever kind of data, photometric or spectroscopic, is considered. The apparent changes of the mean radial velocity (best seen by comparing the four different nights in 1999 – Fig. 2) is not physically real but due to instabilities of the instrument during this run: the measured differences in velocity between the peaks in the thorium spectra for different nights is of the order of 0.3 km s^{-1}. Consequently, the measurements were shifted in order to get the same mean velocity for all the nights. The three nights in 1998 have the same average radial

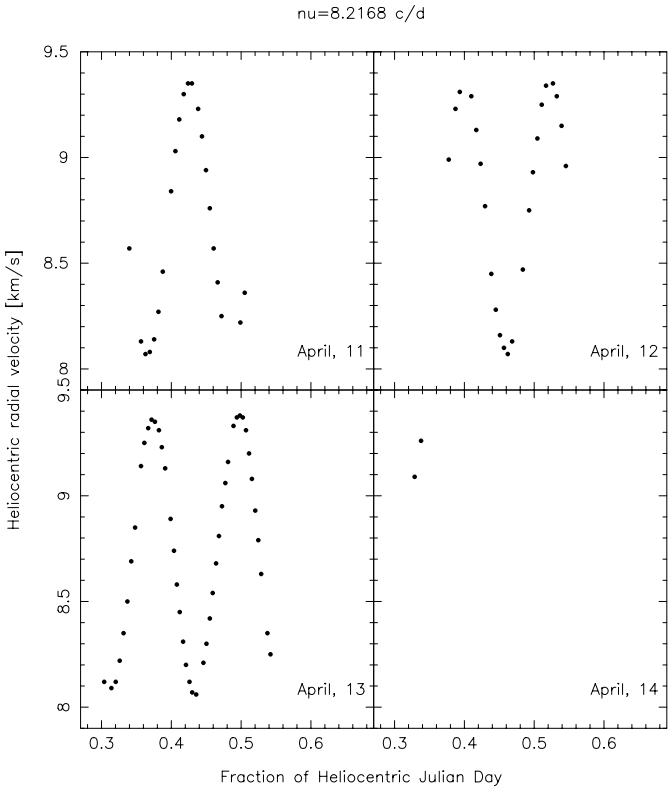

Fig. 1. Heliocentric radial velocity curves associated to the correlation profiles for the 1998 observations.

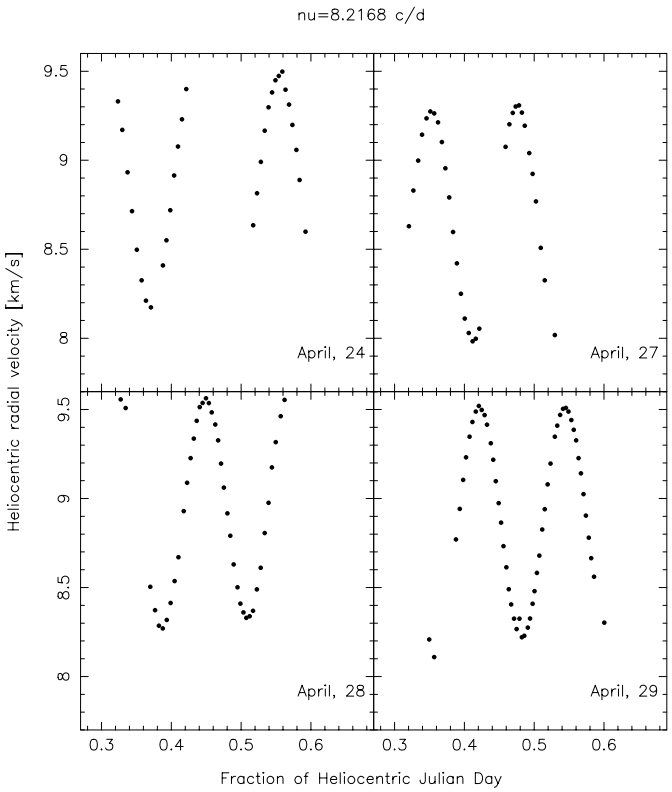

Fig. 2. Heliocentric radial velocity curves associated to the correlation profiles for the 1999 observations.

velocity, so we shifted the data for the four nights in 1999 to the value of the average of the 1998 data.

A sine-fit, performed with the frequency provided by Rodríguez et al. (1998) led to a mean velocity (computed only from the data obtained in 1998) of 8.276 ± 0.007 km s^{-1}, in perfect agreement with the value obtained by Mathias & Aerts (1996). The K semi-amplitude, obtained from the 1998 and the 1999 data, is 0.649 ± 0.007 km s^{-1}, which is slightly larger than the value obtained by Mathias & Aerts (1996) but in agreement with the latter within the 2σ limit. In view of the fact that Mathias & Aerts (1996) only had 17 spectra with a time base of only 3 hours at their disposal, this slightly larger amplitude is no surprise.

Mathias & Aerts (1996) also supposed, from the behaviour of the third velocity moment of the observed profiles (not from the radial velocity), that 20 CVn has at least 2 pulsation periods, but they were unable to find a frequency for the second one. However, from a photometric study, Rodríguez et al. (1998) concluded that 20 CVn definitely is monoperiodic. We performed a frequency analysis on the data obtained in 1998 (the 1999 data were omitted for a frequency search because we had to perform a shift to obtain compatibility) with 4 different methods: Fourier, CLEAN (Roberts et al. 1987), Vanicek (1971) and PDM (Stellingwerf 1978). The results are presented in Fig. 3. The photometric frequency is also clearly present in our new spectroscopic variations. Prewhitening with this frequency leads to flat periodograms. Hence, we re-confirm the monoperiodic character of 20 CVn in the radial-velocity data. A sine-fit performed with the photometric frequency accounts for more than 99.6% of the variability of the radial-velocity data.

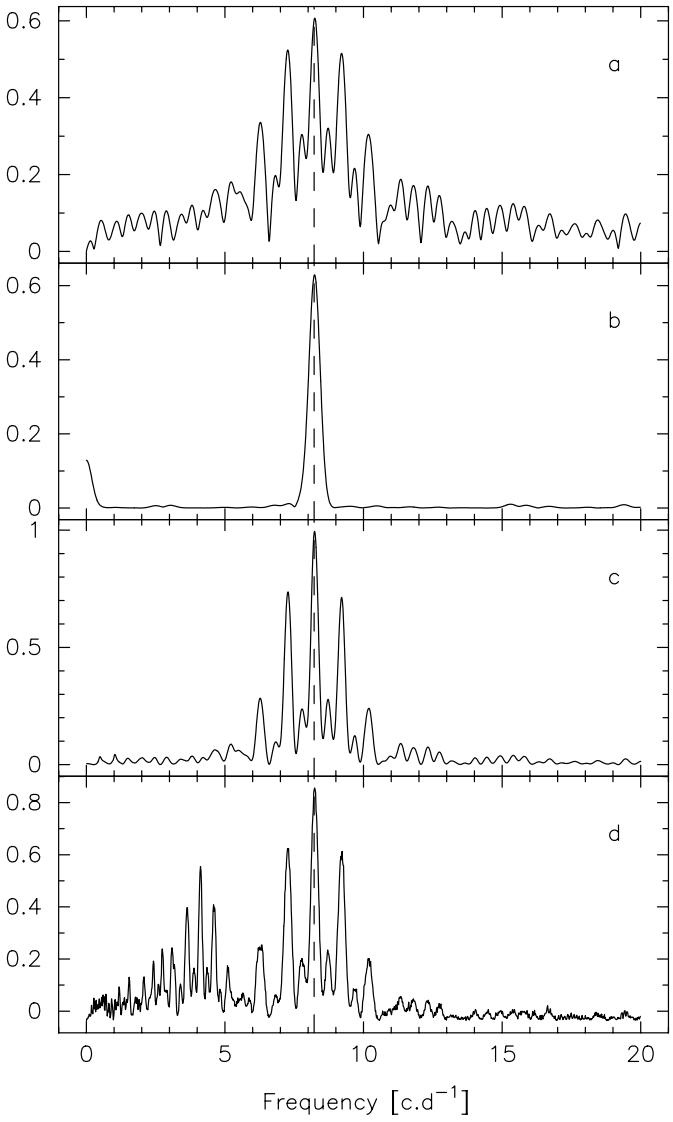

Fig. 3. Frequency analysis performed on the correlation velocity data set obtained in 1998. The vertical dashed line represents the frequency 8.2168 cd^{-1} derived by Rodríguez et al. (1998). **a)** Fourier periodogram. **b)** Power spectrum obtained after 100 iterations with the CLEAN algorithm (with gain 0.5). **c)** Power spectrum obtained from the Vanicek method. **d)** Periodogram obtained from the PDM method with a (5, 2) bin structure; for visual purposes we represented 1-θ.

4. Moment analysis

4.1. The basic steps of a moment analysis

We first briefly recall the basic steps of a mode identification with a moment analysis. In stead of the line profiles themselves, only their first three moments $< v >$, $< v^2 >$ and $< v^3 >$ are considered. As described by Aerts (1996), theoretically $< v >$ can be represented with one term varying with ν, $< v^2 >$ with a constant term plus two terms varying respectively with ν and 2ν, and $< v^3 >$ with three terms varying respectively with ν, 2ν, and 3ν. With the moment method, the first three moment variations of the observed profiles are compared with theoretically calculated moments. A discriminant is set up which measures the deviation of the amplitudes of the observed moments from those of the theoretical moments. Through the theoretical moments, this discriminant is a function of the parameters that appear in the velocity expression due to the non-radial pulsation and rotation of the star: $\ell, m, v_{\rm p}, i, v_\Omega$, and σ. Here, ℓ and m are the wavenumbers of the mode, $v_{\rm p}$ is proportional to the velocity amplitude of the radial component of the pulsation, i is the inclination angle of the star, v_Ω is the projected rotation velocity and σ is the width of the intrinsic profile, assumed to be Gaussian. The horizontal velocity has an amplitude proportional to $(GM/\nu^2R^3)v_{\rm p}$. The discriminant $\Gamma_\ell^m(v_{\rm p}, i, v_\Omega, \sigma)$ is constructed in such a way that the correspondence between theory and observations is best for lower values of Γ.

In practice, the mode identification is carried out as follows. One sets up for each set of wavenumbers (ℓ, m) a grid for the quantities $(v_{\rm p}, i, v_\Omega, \sigma)$. This grid is then exhaustively searched for the parameter set for which the correspondence between theory and observations is best by determining $\gamma_\ell^m \equiv \min_{(v_{\rm p}, i, v_\Omega, \sigma)} \Gamma_\ell^m(v_{\rm p}, i, v_\Omega, \sigma)$. Subsequently, the best set of (ℓ, m) is defined as the one that leads to the lowest γ_ℓ^m-value. For a full description of the method,

we refer to Aerts (1996). We stress, however, that we applied the method to the correlation profiles, and not to the spectral line profiles themselves.

We recall that Mathias & Aerts (1996) already used the moment method on 17 profiles as a test to see if this method gives interpretable results for cross-correlation profiles. They concluded that a non-radial mode corresponds to the main frequency of 20 CVn. They found evidence for an $\ell = 3, m = -2$ mode at low inclination. This conclusion, however, could not be drawn from the moment analysis alone, because the analysis pointed towards different almost equivalent solutions. It was not clear if this was due to the limited data set or to the nature of the intrinsic variability, since some modes closely resemble each other. The best parameter sets found from the moment analysis were therefore taken to calculate theoretical profile variations and to confront the latter with the observed profiles. Only in this way, a mode identification could be made. Although only one consistent solution appeared in this way, it is obvious that the analysis of Mathias & Aerts (1996) calls for a re-evaluation because of the very small data set spread over only one pulsation cycle.

4.2. The observed moments

The three normalised velocity moments of 20 CVn were computed and fitted with a sum of varying terms as described in the previous subsection. In doing so, we took into acccount the fact that the average radial velocity differs slightly for the different nights and we first performed a shift, as already explained in the previous section. This resulted in

$$\begin{cases} < v > \; = [(0.582 \pm 0.003)\sin(\nu t + \psi)]\ \mathrm{km\ s^{-1}}, \\ < v^2 > = \big[(0.24 \pm 0.05)\sin(2\nu t + 2\psi + \frac{3\pi}{2}) \\ \qquad + \ (0.37 \pm 0.05)\sin(\nu t + \psi + \frac{3\pi}{2}) \\ \qquad + \ \ (45.94 \pm 0.04)]\ \mathrm{km^2\ s^{-2}}, \\ < v^3 > = [(0.4 \pm 0.4)\sin(3\nu t + 3\psi) \\ \qquad + \ (0.8 \pm 0.4)\sin(2\nu t + 2\psi + \frac{3\pi}{2}) \\ \qquad + (64.8 \pm 0.4)\sin(\nu t + \psi) \\ \qquad - (42.7 \pm 0.3)]\ \mathrm{km^3\ s^{-3}}. \end{cases} \quad (1)$$

Phase plots of these moments, based on the frequency derived by Rodríguez et al. (1998) are shown in Fig. 4.

We first of all note that the amplitudes determined here have slightly smaller standard errors compared to those given in Mathias & Aerts (1996). Secondly, we remark that the amplitude of $< v >$ differs somewhat from the amplitude of the radial velocity given in Sect. 3. The reason is that the radial velocities mentioned in Sect. 3 were computed by fitting a Gaussian to the line profile, and not by computing the first moment of the profile as is done here. Thirdly, we confirm the very tiny variation of the second moment, which was already noted by Mathias & Aerts (1996). However, $< v^2 >$ does no longer show a clear sinusoidal variation, as was found by Mathias & Aerts (1996). This finding by Mathias & Aerts (1996) was

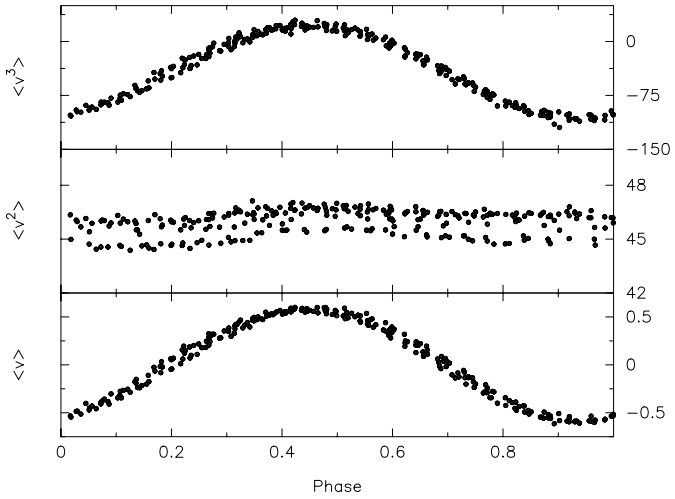

Fig. 4. A phase diagram of the first three observed moments of the correlation profiles of 20 CVn for the frequency 8.216745 $\mathrm{cd^{-1}}$. $< v >, < v^2 >, < v^3 >$ are expressed in respectively km $\mathrm{s^{-1}}$, $\mathrm{km^2\ s^{-2}}$, and $\mathrm{km^3\ s^{-3}}$.

definitely an artefact due to the small number of spectra and the limited time spread. We also note that the constant term of $< v^2 >$ has changed from 40 $\mathrm{km^2\ s^{-2}}$ to 46 $\mathrm{km^2\ s^{-2}}$, which is striking. Finally, a large non-zero constant had to be added to the fitting function of the third moment. This constant has about the same value as the one found by Mathias & Aerts (1996). Since theoretically, for a mono-periodic oscillation, the constant of the third moment is zero, the latter authors concluded that other pulsation modes must be active. However, our current extensive high-quality data set excludes that modes with amplitudes comparable to those of the main mode are present. We therefore have to search for a different explanation for the constant values of $< v^2 >$ and $< v^3 >$.

The strange behaviour of the constants of the second and third moment made us suspicious that this might have something to do with the cross-correlation technique. Intuitively, one might indeed foresee that blended lines result in a too large constant of $< v^2 >$. Their influence on $< v^3 >$ is much harder to predict, since the third moment is a measure of the skewness of the line and so this depends drastically on the position of the two lines which form a blend. We refer to Mathias & Aerts (1996) for a description of the calculation of the cross-correlation profile, but recall here that more than 2000 spectral lines are involved in this calculation. We felt it necessary to check the influence of possible blending with very faint lines to the second moment. In order to do so, we considered one of the cleanest lines in the spectrum of 20 CVn, namely the Fe I line at 6677.987 Å. Our data do not have a sufficiently high S/N ratio to perform a moment analysis on each of the lines separately, since the *amplitudes* of the moments are too noisy to be of any predictive value. On the other hand, a deep absorption line does allow us to determine the *constants* of the moments with a reasonable accuracy, even for a low S/N. We determined the constant

Table 1. A comparison between the different minima of the discriminants of 20 CVn for the correlation profiles without taking into account the constant of $< v^2 >$. γ_ℓ^m, v_p, $(GM/\nu^2 R^3)v_\mathrm{p}$, v_Ω, and σ are given in km s^{-1}.

ℓ	$\lvert m\rvert$	γ_ℓ^m	v_p	$\frac{GM}{\nu^2 R^3}v_\mathrm{p}$	i	v_Ω	σ
3	*2*	*0.09*	*4.5*	*0.27*	*75°*	*6*	*5.0*
0	0	0.12	0.75	–	–	5	6.0
3	*0*	*0.12*	*4.0*	*0.24*	*55°*	*6*	*4.0*
1	1	0.13	1.0	0.06	80°	6	5.0
1	0	0.15	2.0	0.12	70°	6	5.0
3	*1*	*0.15*	*5.0*	*0.30*	*55°*	*5*	*5 .0*
2	0	0.17	1.5	0.09	35°	7	5.5
2	*1*	*0.17*	*3.5*	*0.21*	*80°*	*4*	*5.5*
⋮	⋮	⋮	⋮	⋮	⋮	⋮	⋮

of the second moment of the Fe I $\lambda\lambda$ 6677.987 Å line and obtained 36.5 (km s^{-1})^2. This is significantly smaller than the constant obtained from the cross-correlation function and indicates that we should be very cautious in interpreting the constants of the moments. For this reason, we did not only drop the constant of $< v^3 >$, but we also disregarded the constant of $< v^2 >$ for the mode identification.

4.3. The minima of the discriminant

We adapted the discriminant for mode identification to the situation where only the amplitudes and not the constant given in Eq. (1) are included. As in Mathias & Aerts (1996) we used a stellar radius of 3.31 $R_\odot$ and a mass estimate of 2 $M_\odot$ to compute the amplitude of the horizontal component of the velocity. The linear limb-darkening coefficient was taken to be 0.6. In the calculation of the discriminant, we considered modes with $0 \leq \ell \leq 5$. The parameter grid that we used was: $v_\mathrm{p} = [0.5, 5.0]$ km s^{-1} in steps of 0.5 km s^{-1} (for the radial mode we took a smaller step of 0.05 km s^{-1}); $i = [0°, 90°]$ in steps of 5°; $v \sin i = [4, 8]$ km s^{-1} in steps of 1 km s^{-1}; and $\sigma = [4, 6]$ km s^{-1} in steps of 0.5 km s^{-1}. The discriminant and its minima derived for these grid values and for the amplitudes listed in Eq. (1) for each set (ℓ, m) are listed in Table 1 for the best solutions in parameter space.

Before we interprete Table 1, it is useful to re-evaluate the corresponding table listed in Mathias & Aerts (1996), which we do not repeat here for the sake of brevity. Doing so, we introduce the acronym IACC, which stands for "inclination angle of complete cancellation". Imagine that the star is looked upon in such a way, that the contribution to the observed radial velocity of each point on the stellar disk exactly cancels out the contribution of another point on the stellar disk. As a consequence, the radial velocity curve is flat, i.e. shows no variation in time. Such an inclination angle we call an IACC. In order not to interrupt the flow of the discussion, we consigned a more formal treatment of IACCs to an appendix. It suffices to say that each non-radial pulsation mode has at least one IACC.

The relevance of IACCs to the discriminant minima given by Mathias & Aerts (1996) is that their discriminant turns out to return only modes which are closer than 15° from an IACC (except for the sectoral $\ell = 2$ solution, where the minimum is 26° from the IACC), something which they overlooked. This makes their results somewhat suspect. The discriminant hardly took into account the amplitudes of the 2nd and 3rd moment. The reason is that the discriminant was designed to give moment amplitudes with a larger standard error a lower weight than moment amplitudes with a lower standard error. The relative standard error of the amplitudes of the 2nd and 3rd moment is twice as large as the one of the first moment – see the results listed in their Eq. (3). Consequently, the method had virtually only the first moment to discriminate on, and it had two possibilities to fit the low amplitude of $< v >$: either with a small v_p, or with an inclination angle close to an IACC. However, the grid of Mathias & Aerts (1996) was rather crude in v_p, so that the discriminant had no other choice than to go to an IACC. In such a situation, it is necessary to check if the found solution results in theoretical moment variations that are indeed compatible with the observed ones. Checking fits to the profiles themselves, as Mathias & Aerts (1996) did, is, as we will show later, not sufficient. So far the re-evaluation of the discriminant solutions presented by Mathias & Aerts (1996).

We now take a look at the discriminant based on our much more extended data set of profiles, as listed in Table 1. First of all, the radial mode has a much better classification now than in Mathias & Aerts (1996). The reason is that we used a much smaller step size for the grid of unknowns in the present work than in theirs. In particular, the grid of the amplitude of the radial mode was finer. Unfortunatly, we cannot take such a fine grid into account for all non-radial modes because the computation time becomes unrealistically long. Secondly, here again, we find several solutions closer than 15° to an IACC. These are indicated in italic in Table 1. Although we have much smaller relative standard errors for all the amplitudes of the moments, the one of the first moment is still significantly smaller than the one of the other amplitudes. We also mention that we find this time also solutions which are not close to an IACC.

4.4. Comparison of theoretical and observed profiles

In order to check thoroughly the possibilities found by the discriminant, we generated theoretical line profiles for the parameters listed in Table 1, allowing to change slightly the found values for $v_\mathrm{p}, i, v_\Omega, \sigma$ in order to find the best correspondence with the observed profiles. To quantify the latter condition, we introduce a goodness-of-fit parameter Σ in the following way. We performed the comparison with time series of 20 normalized observed profiles, each consisting of 41 pixels. They were chosen

Table 2. A comparison between the different pulsation models that result in the best goodness-of-fit values Σ of 20 CVn. Σ_ℓ^m is a dimensionless quantity, while $v_{\rm p}$, $(GM/\nu^2R^3)v_{\rm p}$, v_Ω, and σ are given in km s^{-1}.

ℓ	m	Σ_ℓ^m	$v_{\rm p}$	$\frac{GM}{\nu^2R^3}v_{\rm p}$	i	v_Ω	σ
2	0	0.0022	2.5	0.15	45°	4	5.5
3	0	0.0022	2.0	0.12	25°	4	5.7
0	0	0.0023	0.85	0.05	–	7	5.0
3	+1	0.0024	2.5	0.15	85°	6	5.5
4	+4	0.0026	1.5	0.09	70°	6	5.5
3	+2	0.0026	3.0	0.18	15°	6	5.5
3	−2	0.0027	3.0	0.18	15°	4	5.5
2	+1	0.0029	2.0	0.12	90°	4	5.5
⋮	⋮	⋮	⋮	⋮	⋮	⋮	⋮

in such a way that they are approximately equidistant in pulsation phase. These observed profiles are shown as open circles in Fig. 5. We next calculate the average deviation (Σ) per wavelength pixel between theoretically-determined and observed line profiles:

$$\Sigma \equiv \frac{1}{20}\sqrt{\frac{1}{40}\sum_{i=1}^{41}(I_{i,\rm obs}-I_{i,\rm th})^2}, \qquad (2)$$

in which the subscripts "obs" and "th" denote the "observed" and "theoretical" values of the normalized flux in the ith wavelength pixel of the profile. The more likely the mode, the smaller Σ. We determined Σ for all the (ℓ, m) combinations and with parameters close to the ones listed in Table 1. The results for the best combinations (i.e. lowest Σ) are given in Table 2. It can be seen that many equivalent solutions can be found, so that the predictive power of fitting is small. Two of the better solutions are shown as full lines in Fig. 5. We show there the comparison between the observed profiles (open circles) and those obtained with the parameters given in Table 2 (full lines) for a solution close to an IACC and one far from an IACC. The other non-radial solutions (e.g. $\ell = 3, m = 2$) listed in Table 2 give very comparable fits to the data.

Interesting are the corresponding moments predicted by these theoretical profiles, which are shown in the lower panels of Fig. 5 with the same scale as the observed ones shown in Fig. 4. We observe that the moment variations of non-radial modes are either far too small compared to the observed ones and/or that the second moment shows a large variation (of sinusoidal shape for the sectoral mode and of a double sine for the zonal mode). We find the same result for all the other modes listed in Table 2: there is always at least one property of the observed moments that is not explained by the non-radial solutions. We therefore must conclude that the seemingly good fits given in the top panels are misleading since they lead to an inaccurate prediction of the moment values. In the right panel of Fig. 5, we show the best solution for the radial mode. It occurs for an amplitude of 0.85 km s^{-1}, $v \sin i = 7$ km s^{-1} and $\sigma = 5$ km s^{-1}, leading to $\Sigma = 0.0023$. It can be seen that the fitting profiles are of the same quality as those for the non-radial ones shown in the other panels. Moreover, the variations of the theoretical moments that belong to this solution *do* look very much like the observed ones (see lower panel of Fig. 5). Even the constant of the second moment has the correct value. We therefore conclude that 20 CVn exhibits a radial pulsation.

How can it be that Mathias & Aerts (1996), who applied the same mode identification technique on data of the same instrument, obtained a different result? Several reasons can be found and we summarize them once more. Firstly they interpreted the non-zero constant of their third moment as coming from a second mode which they could not resolve with their small data set of 17 datapoints spanning only about 3 hours. The higher-quality data set with a longer time-base presented in this paper rules out this interpretation. Secondly, their moment analysis did not favour the radial mode. This is partly due to the fact that the grid they used to scan the mode parameter space (in particular in the $v_{\rm p}$ direction) turned out to be too coarse, and partly because the moment method performs poorly when the number of data points is low, in the sense that many almost equally probably solutions appear (De Pauw et al. 1993). Moreover, they used line profile fitting to choose between the candidate solutions of their moment analysis, but it was shown above that the predictive power of line profile fits is small in the case of 20 CVn.

5. Discussion

Our analysis of new spectroscopic observations shows that the radial velocity varies sinusoidally with one frequency which accounts for more than 99.6% of the variance. So we confirm the mono-periodic character of the pulsation found photometrically by Rodríguez et al. We also confirm both the mean radial velocity and amplitude variations measured by Mathias & Aerts (1996).

We conclude that only the radial mode is able to fit both the observed moment variations and the observed lined profile variations. Our study thus solves the controversy between the photometric and spectroscopic behaviour of 20 CVn, since we fully agree with the identification of a radial mode, as proposed by Rodríguez et al. (1998).

Just as Rodríguez et al. (1998), we also experienced that identifying the mode of 20 CVn unambiguously is not easy, despite the fact that the star is mono-periodic. This can be ascribed to the low amplitude of the mode. From a moment analysis using all three moments it was hardly possible to distinguish the radial mode from some other non-radial modes. This was caused by the large relative error of the amplitudes of the 2nd and the 3rd moment so that the method focused on the 1st moment. In addition, the special properties of the spherical harmonics which are viewed upon a certain angle also contributed to

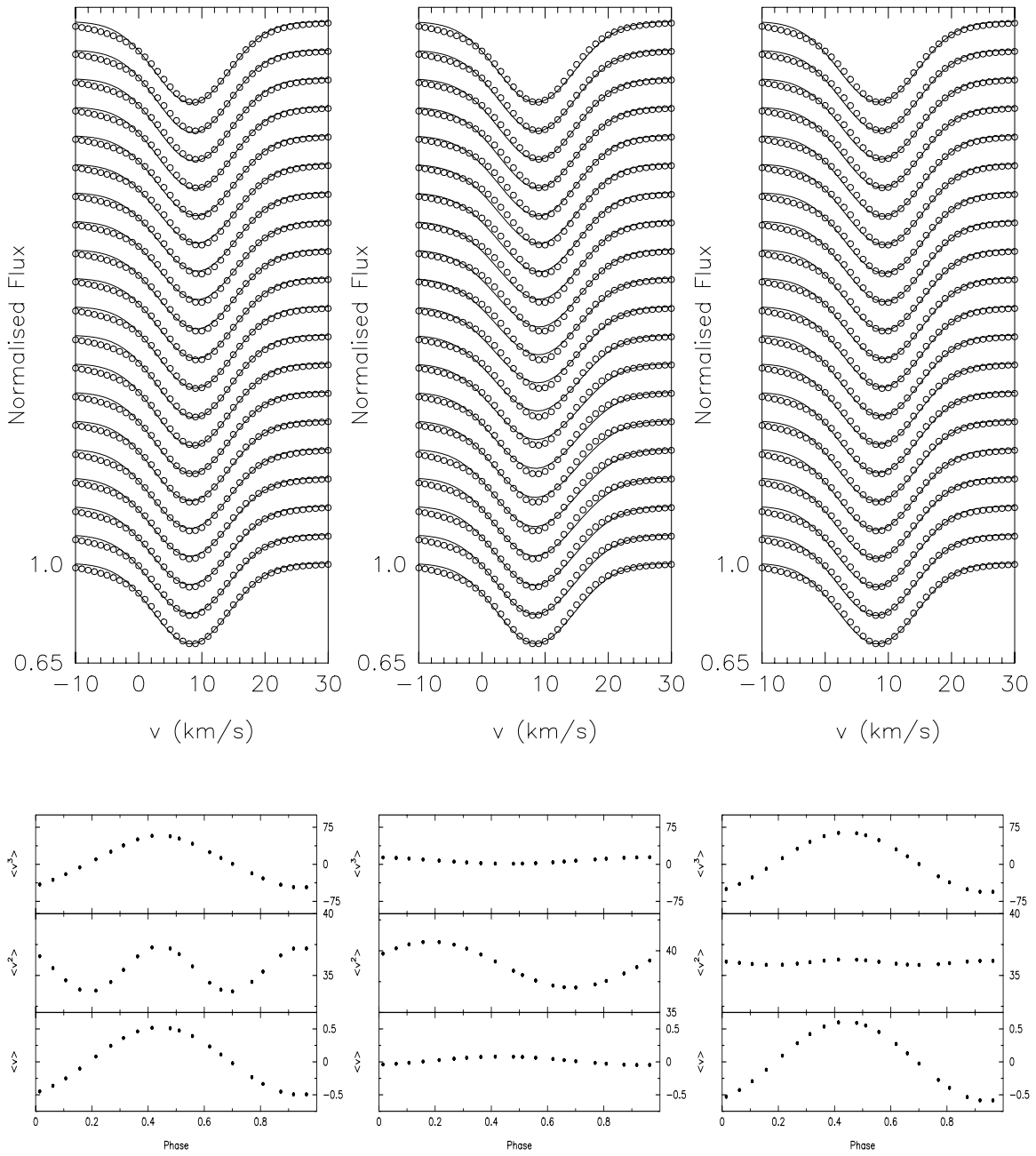

Fig. 5. Top: a comparison between theoretical profiles generated with the parameters listed in Table 2 (full line) and observed profiles (open dots). The left panel shows the solution for $(\ell, m) = (2, 0)$, the middle one for $(4, +4)$, and the right one for the radial mode. Bottom: the variations of the moments corresponding to the theoretical profiles shown in the top panels.

the confusion. Line profile fitting resulted in a list of indistinguishable candidate solutions too (including the radial mode). Some fits were rather good in the center but less good in the wings, or vica versa. Globally, many parameter sets had the same goodness of fit as the radial mode. We then concentrated on the variation of the width of the line profile (i.e. the second moment). The observed amplitudes of the 2nd moment have a large relative uncertainty, but it was the smallness of these amplitudes that could be exploited. Only the radial mode was able to mimic the small variation of the 2nd moment while still producing a radial velocity amplitude of about 0.5 $\mathrm{km\,s^{-1}}$.

We also conclude from our study that using cross-correlation curves in the analysis of pulsating stars is possible and opens new possibilities. Taking a standard cross-correlation technique is fine when one wants to derive accurate frequencies and radial velocities. Using the profiles for mode identification needs, however, a more tedious approach since the automatic routines used to avoid blended lines are not sufficiently accurate for this purpose. For mode identification, one should in any case not interprete the constant values of the higher-order moments. A more sophisticated way to determine the cross-correlation function is to calculate it by means of only very few

absorption lines that are carefully selected for each star individually, so that blended lines are definitely excluded.

Appendix A: Inclination angles of complete cancellation

A non-radially pulsating star does not necessarily show a time-varying radial velocity curve (or equivalently first moment), even in the case of a monoperiodic low-degree pulsator. To investigate this more thoroughly, we model the first moment $< v >$ in the definition used in this paper, i.e. assuming that the time dependence of the observed line profile is solely due to this velocity field, and neglecting any other time dependence like stellar surface temperature variations. We adopt a linear limb-darkening law with coefficient u. For such assumptions, we recall the expression for the first moment as given in Aerts et al. (1992) and write it in a slightly different form:

$$\begin{aligned} < v > &= v_{\rm p}\ A(\ell,m,i)\ \sin(\nu t+\psi) \\ &\equiv \mathcal{A}(\ell,v_{\rm p},u)\ a_{\ell,m,0}(i)\ \sin(\nu t+\psi), \end{aligned} \tag{A.1}$$

where

$$\mathcal{A}(\ell,m,i) \equiv \frac{2N_\ell^m v_{\rm p}}{1+\frac{2}{3}\frac{u}{1-u}}\left(J^0_{\ell,0}+KH^0_{\ell,0}\right). \tag{A.2}$$

For the sake of completeness, we list again the definitions of the integrals

$$J^n_{\ell,k} \equiv \int_0^1 (\mu^2+\beta\mu^3)(1-\mu^2)^{n/2}P_\ell^k {\rm d}\mu \tag{A.3}$$

and

$$\begin{aligned} H^n_{\ell,k} \equiv\ & (\ell+1)\int_0^1 (1-\mu^2)^{n/2}[(\mu^2+\beta\mu^3)P_\ell^k \\ & -(\mu+\beta\mu^2)P^k_{\ell+1}]{\rm d}\mu. \end{aligned} \tag{A.4}$$

The only difference with the description given by Aerts et al. (1992), is that we isolated the function $a_{\ell,m,0}(i)$ in the expression for the first moment. This function is a particular case of the more general spherical harmonic transformation coefficients $a_{\ell,m,k}(i)$, which are used to express the pulsational velocity field in a reference system where the z-axis is pointing towards the observer:

$$\begin{aligned} a_{\ell,m,k}(i) \equiv\ & (\ell+m)!(\ell-m)! \\ & \times\sum_r \frac{(-1)^{\ell+k+r}\ \sin(i/2)^{2\ell-2r-m-k}\cos(i/2)^{2r+m+k}}{r!(m+k+r)!(\ell-m-r)!(\ell-k-r)!} \end{aligned} \tag{A.5}$$

with $r\geq 0$, $r\geq -k-m$, $r\leq \ell-m$, $r\leq \ell-k$.

The reason why we isolated the function $a_{\ell,m,0}(i)$ is the following. The function $\mathcal{A}(l,v_{\rm p},u)$ in general becomes smaller for higher degree ℓ. This represents the so-called partial cancellation effect. The higher ℓ, the more sectors and/or zones divide the stellar surface, neighbouring regions having opposite velocity sign. Their influence on the line-profile variability therefore tends to partially cancel out. The factor $\mathcal{A}$ does not depend on the inclination angle nor on the azimuthal number m: only the total number of nodal lines is relevant, not their configuration.

Table A.1. A list of inclination angles of complete cancellation for all non-radial modes with $\ell\leq 5$ and $m\geq 0$.

(ℓ,m)	IACC				
$(1,0)$					90°
$(2,0)$			54.7°		
$(3,0)$		39.2°			90°
$(4,0)$		30.6°		70.1°	
$(5,0)$	25.0°		57.4°		90°
$(1,1)$	0°				
$(2,2)$	0°				
$(3,3)$	0°				
$(4,4)$	0°				
$(5,5)$	0°				
$(2,1)$	0°				90°
$(3,1)$	0°			63.4°	
$(3,2)$	0°				90°
$(4,1)$	0°	49.1°			90°
$(4,2)$	0°			67.8°	
$(4,3)$	0°				90°
$(5,1)$	0°	40.1°		73.4°	
$(5,2)$	0°		54.7°		90°
$(5,3)$	0°			70.5°	
$(5,4)$	0°				90°

For *each* non-radial pulsation mode there exists *at least one* inclination angle i^* so that the function $a_{\ell,m,0}(i)$ is zero. We define i^* as an *inclination angle of complete cancellation*, or abbreviated IACC. In the case of complete cancellation the star is looked upon in such a way that the contribution to the observed radial velocity of each point on the stellar disk exactly cancels out the contribution of another point on the stellar disk.

From Eq. (A.5) one can derive the following properties of the function $a_{\ell,m,0}(i)$:

1. if i^* is an IACC of the mode (ℓ,m), then $180^\circ-i^*$ and $360^\circ-i^*$ are also IACCs of this mode;
2. the mode (ℓ,m) has the same IACCs as the mode $(\ell,-m)$;
3. $i^*=0^\circ$ is an IACC for a zonal mode $(\ell,0)$;
4. $i^*=90^\circ$ is an IACC for a zonal mode with odd degree ℓ;
5. $i^*=k\ 90^\circ$ with k an integer, is an IACC for the modes $(\ell,-\ell+1)$ and $(\ell,\ell-1)$ for $\ell\geq 2$.

In Table A.1 we list all IACCs lower than 90° for all non-radial modes with $\ell\leq 5$ and $m\geq 0$.

For the sake of completeness, we still mention two useful properties of IACCs. Firstly, for high-degree sectoral modes the derivative of $a_{\ell,m,0}(i)$ at the IACCs $i^*=0^\circ$ and $i^*=180^\circ$ becomes very small, so that we can speak of an *interval* of inclination angles of (almost) complete cancellation rather than of one IACC. Secondly, Eq. (A.1) is

easily generalised for multiperiodic stars as the sum of the contributions of each of the individual modes (see Mathias et al. 1994). This can have interesting implications for rotational frequency multiplets obtained from radial velocity data. It might e.g. happen that a multiplet misses two peaks as the inclination angle of the star may be an IACC of the contributing modes $(\ell, \pm m)$. Finally, we note that an IACC is defined as the inclination angle for which the first moment (or equivalenty, the radial velocity curve) shows no time variation. Its definition does not concern the time dependence of the higher order moments of a line profile.

References

Aerts, C. 1996, A&A, 314, 115

Aerts, C., de Pauw, M., & Waelkens, C. 1992, A&A, 266, 294

Baranne, A., Mayor, M., & Poncet, J. L. 1979, Vistas Astron., 23, 279

Baranne, A., Queloz, D., Mayor, M., et al. 1996, A&AS, 119, 373

Bradley, P. A., & Guzik, J. A. 2000, The Impact of Large-Scale Surveys on Pulsating Star Research, ed. L. Szabados, & D. W. Kurtz, ASP Conf. Ser., 203

Breger, M. 2000, Delta Scuti and Related Stars, ed. M. Breger, & M. H. Montgomery, ASP Conf. Ser., 210

De Pauw, M., Aerts, C., & Waelkens, C. 1993, A&A, 280, 493

Garrido, R., García-Lobo, E., & Rodríguez, E. 1990, A&A, 234, 262

Gautschy, A., & Saio, H. 1996, ARA&A, 34, 551

Mathias, P., & Aerts, C. 1996, A&A, 312, 905

Mathias, P., Aerts, C., de Pauw, M., Gillet, D., & Waelkens, C. 1994, A&A, 283, 813

Roberts, D. H., Lehár, J., & Dreher, J. W. 1987, AJ, 93, 968

Rodríguez, E., Rolland, A., Garrido, R., et al. 1998, A&A, 331, 171

Rodríguez, E., López de Coca, O., Rolland, A., Garrido, R., & Costa, V. 1994, A&AS, 106, 21

Stellingwerf, R. F. 1978, ApJ, 224, 953

Templeton, M. R., Bradley, P. A., & Guzik, J. A. 2000, ApJ, 528, 979

Vanicek, P. 1971, Ap&SS, 12, 10